ENVIRONMENTAL RESEARCH
CLIMATE

LETTER

Comparing the impacts of ozone-depleting substances and carbon dioxide on Arctic sea ice loss

Mitchell Bushuk[1,*], **Lorenzo M Polvani**[2,3] and **Mark R England**[4]

[1] National Oceanic and Atmospheric Administration/Geophysical Fluid Dynamics Laboratory, Princeton, NJ, United States of America
[2] Department of Applied Physics and Applied Mathematics, Columbia University, New York, NY, United States of America
[3] Lamont Doherty Earth Observatory, Columbia University, Palisades, NY, United States of America
[4] University of California Santa Cruz, Santa Cruz, CA, United States of America
[*] Author to whom any correspondence should be addressed.

E-mail: mitchell.bushuk@noaa.gov

Keywords: Arctic sea ice, polar climate change, ozone-depleting substances, climate change ensembles

Supplementary material for this article is available online

OPEN ACCESS

RECEIVED
6 March 2023

REVISED
16 July 2023

ACCEPTED FOR PUBLICATION
4 August 2023

PUBLISHED
4 September 2023

Abstract

The rapid decline of Arctic sea ice is widely believed to be a consequence of increasing atmospheric concentrations of greenhouse gases (GHGs). While carbon dioxide (CO_2) is the dominant GHG contributor, recent work has highlighted a substantial role for ozone-depleting substances (ODS) in Arctic sea ice loss. However, a careful analysis of the mechanisms and relative impacts of CO_2 versus ODS on Arctic sea ice loss has yet to be performed. This study performs this comparison over the period 1955–2005 when concentrations of ODS increased rapidly, by analyzing a suite of all-but-one-forcing ensembles of climate model integrations, designed to isolate the forced response to individual forcing agents in the context of internal climate variability. We show that ODS have played a significant role in year-round Arctic sea ice extent and volume trends over that period, accounting for 64% and 32% of extent and volume trends, respectively. These impacts represent 50% and 38% of the impact from CO_2 forcing, respectively. We find that ODS act via similar physical processes to CO_2, causing sea ice loss via increased summer melt, and not sea ice dynamics changes. These findings imply that the future trajectory of ODS emissions will play an important role in future Arctic sea ice evolution.

1. Introduction

Observations of Arctic sea ice extent (SIE) and volume (SIV) have documented a precipitous sea ice decline over the satellite era (Stroeve and Notz 2018, Meredith *et al* 2019). While internal climate variability has played a non-negligible role in observed Arctic sea ice loss (e.g. Kay *et al* 2011, Stroeve *et al* 2012, Notz 2015, Ding *et al* 2019, England *et al* 2019), the recent IPCC AR6 concluded that it is *very likely* that anthropogenic forcing due mainly to greenhouse gases (GHGs) is responsible for more than half of the observed summer sea ice loss (IPCC 2023). Carbon dioxide (CO_2) is the dominant source of anthropogenic GHG radiative forcing, and thus much of the sea ice community's work has focused on the sea ice response to CO_2 emissions (e.g. SIMIP Community 2020). However, recent work has highlighted that other anthropogenic GHG forcing agents—particularly ozone-depleting substances (ODS)—also played a substantial role in Arctic sea ice loss (Polvani *et al* 2020, Sigmond *et al* 2023).

ODS are halogenated carbon compounds (e.g. chlorofluorocarbons), which were developed for use as refrigerants, aerosol propellants, and solvents. The substantial emission of ODS into the atmosphere began in the 1950s and continued to increase unabated until the signing of the Montreal Protocol in 1987, which strongly regulated their use (World Meteorological Organization 2018). ODS are well known as the primary driver of stratospheric ozone (O_3) depletion and the cause of the Antarctic ozone hole (Solomon 1999). Less well known are the direct impacts of ODS on the climate system via radiative forcing. ODS are long-lived

gases with powerful radiative efficiencies: For example, CFC-11 and CFC-12 have 20-year global warming potentials roughly 10 000 times that of CO_2 (World Meteorological Organization 2018). Thus, despite their relatively low concentrations compared to CO_2, ODS have a notable radiative forcing (Ramanathan 1975, Montzka *et al* 2011). Specifically, over the period 1955–2005 where ODS concentrations increased rapidly, the radiative forcing from ODS was 0.31 W m^{-2} (Meinshausen *et al* 2011). This represents 30% of the CO_2 forcing over this period (1.02 W m^{-2}) and a slightly larger forcing than methane (0.23 W m^{-2}; based on abundance changes), making ODS an important contributor to GHG forcing over the second half of the 20th century.

A number of earlier studies have examined the so-called 'World Avoided' by the signing of the Montreal Protocol, showing that the reductions in ODS emissions since 1987 have resulted in a substantial decrease in surface climate warming (Hansen *et al* 1989, Velders *et al* 2007, Morgenstern *et al* 2008, Garcia *et al* 2012, Polvani *et al* 2016, Goyal *et al* 2019) and Arctic sea ice loss (England and Polvani 2023). Recently, Polvani *et al* (2020) investigated a related but distinct question: how much of the historical climate change that has already been observed can be attributed to historical forcing from ODS? They found that when ODS are kept fixed at 1955 levels in the CESM1 climate model, Arctic September SIE loss and annual-mean Arctic surface air temperature (SAT) warming are only *one half* of those in the historical integrations (in which ODS concentrations increase markedly over the second half of the 20th century). In recent analogous experiments performed with the CanESM5 model, Sigmond *et al* (2023) also found that September SIE loss and Arctic warming are roughly one half of those in historical integrations.

The impacts from ODS on sea ice loss found by Polvani *et al* (2020) are remarkably large. Their surprising result, however, is in part related to the large cancellation that occurs between the warming effects of CO_2 and the cooling effects of aerosols over the second half of the twentieth century (e.g. Fyfe *et al* 2013, Kong and Liu 2023), which tends to highlight the impacts of ODS compared to this residual. Therefore, in order to better understand the impact of ODS on Arctic sea ice loss, it is necessary to (i) directly compare the impacts of ODS and CO_2; and (ii) understand the physical mechanisms contributing to the differences in sea ice trends. In this work, we address these topics by analyzing all-but-one-forcing climate model ensembles in which ODS and CO_2 are respectively held fixed at their 1955 levels and compared to a historical forcing ensemble. We use large ensembles for this study in order to robustly evaluate the forced response of sea ice to different forcing agents in the context of internal climate variability. We first quantify the monthly impacts of ODS on a range of sea ice variables and directly compare these with the impacts of CO_2 forcing. We then consider the physical processes contributing to the sea ice trend differences, analyzing sea ice mass budgets, Arctic surface energy budgets, and sea ice sensitivity across the experiments. Finally, we discuss the implications of these findings for past and future simulations of Arctic climate change.

2. Methods

2.1. Model experiments

This study is based on a multi-forcing suite of single-model initial condition large ensembles (SMILEs) run using the Community Earth System Model version 1 with the Community Atmosphere Model, version 5 (CESM1(CAM5); Hurrell *et al* 2013). Our baseline SMILE is the widely-used CESM1-LE (Kay *et al* 2015), which is a 40-member ensemble that uses CMIP5 historical radiative forcings from 1920–2005. The initial conditions for the CESM1-LE are nearly identical, differing only by roundoff-level perturbations in their atmospheric initial states. We select 10 members from this ensemble from which forcing perturbation experiments are branched in 1955. We refer to this 10-member ensemble of historical simulations as the 'All' forcing ensemble.

In addition, we here analyze three 10-member ensembles spanning 1955–2005, in which certain forcing agents are held fixed at 1955 levels. Specifically, we run '$FixCO_2$', 'FixODS', and '$FixODSO_3$' ensembles, which respectively fix the CO_2, ODS, and ODS and O_3 concentrations at their 1955 levels. In these fixed-forcing experiments, all other forcing agents are specified to evolve according to their time-varying historical values. This 'all-but-one-forcing' approach allows one to directly quantify the impact of given forcings via comparison to the historical runs, and assuming a linear response. It is widely used in climate science (e.g. Polvani *et al* 2011, Deser *et al* 2020).

For readers unfamiliar with ODS, we briefly note that these compounds include chlorofluorocarbons, hydrochlorofluorocarbons, halons, carbon tetrachloride, methyl chloride, methyl chloroform, and others. CAM5 specifies the concentrations of two ODS forcing agents, CFC-11* and CFC-12, which are time-varying and 'well-mixed', i.e. with the same value for all latitudes, longitudes, and vertical levels. CFC-11* is a linear combination of CFC-11 and 25 other halocarbons, weighted by their radiative efficiency

relative to CFC-11. For the FixODS experiments, CFCs and related halocarbons are held fixed at their 1955 values and for the FixODSO$_3$ experiments both ODSs and stratospheric O$_3$ are held fixed at their 1955 values. For simplicity, following Prather *et al* (2011) and Young *et al* (2013), stratospheric ozone is defined as concentrations in excess of 150 ppbv; this approach avoids having to specify a tropopause height at each horizontal grid point in the model.

Also, we recall that the output from these same four CESM1(CAM5) model ensembles have previously been analyzed by Liang *et al* (2022), who evaluated their SAT and September sea ice responses and reported how different climate feedbacks in the Arctic result in a larger Arctic Amplification from ODS than from CO_2 forcing in this model. The present paper, instead, focuses on sea ice itself: we here examine both the extent and volume trends, spatial patterns of the forced response, and perform a mass and energy budget of the sea ice field to determine whether ODS and CO_2 impact sea ice via different mechanisms. A careful analysis of the Arctic sea ice response to ODS, and its comparison to the response to CO_2, has not been performed to date.

2.2. Comparison methodology

In order to isolate the forced response, we focus our analysis on ensemble-mean trends across the multi-forcing ensemble. Ensemble-mean trends are obtained by first computing the ensemble mean of a given quantity (e.g. Pan-Arctic SIE) and then computing the linear trend of this ensemble mean. We estimate a 95% confidence interval for the ensemble-mean trends using a bootstrapping approach in which the ensemble is repeatedly resampled (with replacement) in order to produce an empirical distribution of ensemble-mean trends based on 1000 realizations.

The statistical significance of trend differences between two ensembles are assessed using the bootstrapped distributions of trends. The standard errors in ensemble-mean trends are added in quadrature to obtain a standard error for the trend difference. If the trend difference exceeds 1.96 standard errors, the difference is considered statistically significant at the 95% confidence level.

We assess the fidelity of simulated trends by comparing to monthly-averaged passive microwave satellite SIC observations from the National Snow and Ice Data Center (NSIDC) processed using the NASA Team retrieval algorithm (data set ID: NSIDC-0051, Cavalieri *et al* 1996). We focus our analyses on the time period 1979–2005, since this allows for direct comparison to observations and also is the time period that shows the largest differences between experiments. Computing trends over the period 1955–2005 does not change the qualitative findings of this study. For sea ice thickness and volume, we do not compare to an observational estimate due to the lack of a continuous thickness observational record over this time period.

3. Results

3.1. Impact of ODS and CO_2 on Arctic sea ice trends

We first consider the relative impacts of ODS and CO_2 on Arctic sea ice trends. Figure 1 shows simulated ensemble-mean SIE timeseries across the multi-forcing ensemble. For both March and September SIE, the ensemble-mean trends are relatively indistinguishable over the period 1955–1975, and begin to show differences over the period 1975–2005. Consistent with earlier work (e.g. Swart *et al* 2015), we find that the All forcing ensemble simulates ensemble-mean SIE trends that are in reasonably good agreement with observations. The observed trends are generally lower than the ensemble-mean trends, but fall within the distribution of simulated trends in most non-winter months of the year (not shown). The modeled winter SIE trends are higher than observed, potentially related to underestimated trends in ocean heat transport into the Arctic Ocean (Li *et al* 2017).

Fixing CO_2 at 1955 levels has a striking impact on simulated SIE, as expected from its dominant contribution to GHG forcing (Meinshausen *et al* 2011). For both summer and winter SIE, we find that the fixed CO_2 simulations exhibit relatively flat SIE evolutions over the simulation period. This suggests that in CESM1(CAM5) the cooling effects of aerosol forcing and land use roughly balance the warming effects of non-CO_2 GHGs over this period. ODS and O$_3$ are two of these non-CO_2 GHGs: note, however, that the former are well mixed, but not the latter. For both September and March SIE, we find that the FixODS run lies roughly halfway between the All and FixCO_2 runs, indicating that ODS have made a substantial contribution to Arctic sea ice loss over the late 20th century. With the exception of a winter SIE anomaly in the 1970s, the FixODSO$_3$ runs show a similar SIE evolution to FixODS, indicating that the contribution of stratospheric O$_3$ to SIE trends is minimal relative to ODS.

A comparison of monthly ensemble-mean trends in SIE and SIV is shown in figure 2. We find that fixing ODS forcing causes a substantial reduction in simulated SIE trends in all months of the year, with the All forcing trends being reduced by 64% in the annual mean (compare blue and green bars; monthly SIE trends are reduced by 40%–94%). The SIE trend differences between the FixODS and All forcing ensembles are statistically significant in 8 months of the year (insignificant differences in Jan, Apr, May, June). We find that

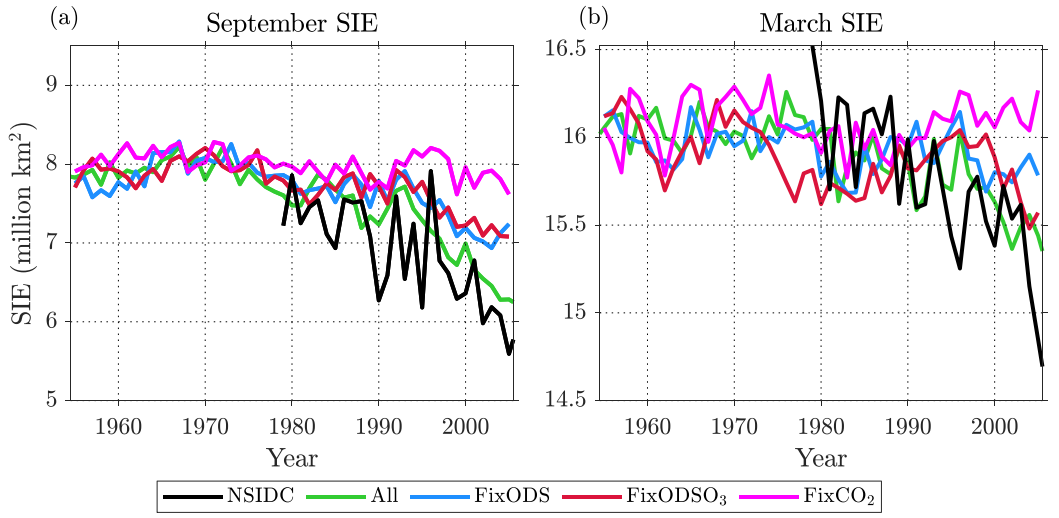

Figure 1. Observed (black lines) and simulated ensemble mean (colored lines) time series of (a) September and (b) March pan-Arctic sea ice extent (SIE) in the All forcing (green), FixODS (blue), FixODSO$_3$ (red), and FixCO$_2$ (magenta) simulations.

additionally fixing O_3 has only a small impact on SIE trends (compare red and blue bars), and that the SIE trend differences between the FixODSO$_3$ and FixODS ensembles are not statistically significantly different in any month of the year. As one would expect, fixing CO_2 has the largest impact on SIE trends, eliminating or even reversing the trends present in the All forcing run (compare magenta and green bars). The average trend reduction from fixing CO_2 is 127% of the All forcing trends (monthly trends are reduced by 88%–170%), and these trend differences are statistically significant in all months of the year.

ODS and CO_2 also have clear impacts on SIV trends (figure 2(b)), however the quantitative trend reductions differ from the SIE trends. In particular, fixing ODS results in an average 32% reduction in SIV trends relative to the All forcing run, whereas fixing CO_2 results in an average 84% reduction. SIV trends also show a more clear separation between the FixODSO$_3$ and FixODS ensembles, however these differences are not statistically significant in any month of the year. The FixCO$_2$ and FixODSO$_3$ SIV trends have statistically significant differences with the All forcing ensemble in all months of the year, whereas the FixODS differences are only significant in 5 months of the year (insignificant differences in January–July).

The fixed ODS and CO_2 ensembles allow us to perform a direct 'head-to-head' comparison of their impacts on Arctic sea ice loss. The global radiative forcing from ODS over the period 1955–2005 is 0.31 W m^{-2}, which is 30% of the radiative forcing from CO_2 over the same period (1.02 W m^{-2}; Meinshausen *et al* 2011). Thus, a reasonable null hypothesis would be for the impact of ODS on sea ice loss to be 30% that of CO_2. However, we find that ODS have an outsized impact on Arctic sea ice loss relative to this expectation, with impacts on SIE and SIV trends that are 50% and 38% of the CO_2 impact, respectively. This finding is consistent with the results of Liang *et al* (2022), who reported that ODS also produce larger Arctic amplification than CO_2.

To provide a more complete picture of the response of sea ice to ODS and CO_2, in figures 3 and S1 we plot spatial trends across the experiments, which show coherent behavior across a range of sea ice variables. We show summer spatial trends in figure 3, as these are the months with the largest impacts from ODS, and show winter spatial trends in the supplementary material (figure S1). Relative to the FixCO$_2$ and FixODS simulations, the All forcing run shows trends towards less extensive (row (a)), thinner (row (b)), and younger (row (d)) sea ice in both the summer and winter seasons. The All forcing runs also shows trends towards less snow on sea ice (row (c)) and warmer SAT (row (e)) in both summer and winter. The spatial trend patterns are broadly consistent across the experiments, with the trends becoming progressively more muted as ODS, ODSO$_3$, and CO_2 are respectively held fixed. In both summer and winter, the SIC trend differences occur near the ice-edge location (row (a)), whereas the sea ice thickness (SIT; row (b)), snow depth (SND; row (c)), and SAT (row (e)) trend differences occur throughout the Arctic Ocean domain, suggesting that a common broad-scale mechanism is driving the trend differences. The sea ice age differences (row (d)) also occur throughout the Arctic basin and are intensified along the pathway of the transpolar drift stream. The summer SIC differences are relatively zonally symmetric around the summer sea ice edge location, whereas the winter SIC differences are largest in the Barents and Greenland Seas and the Sea of Okhotsk.

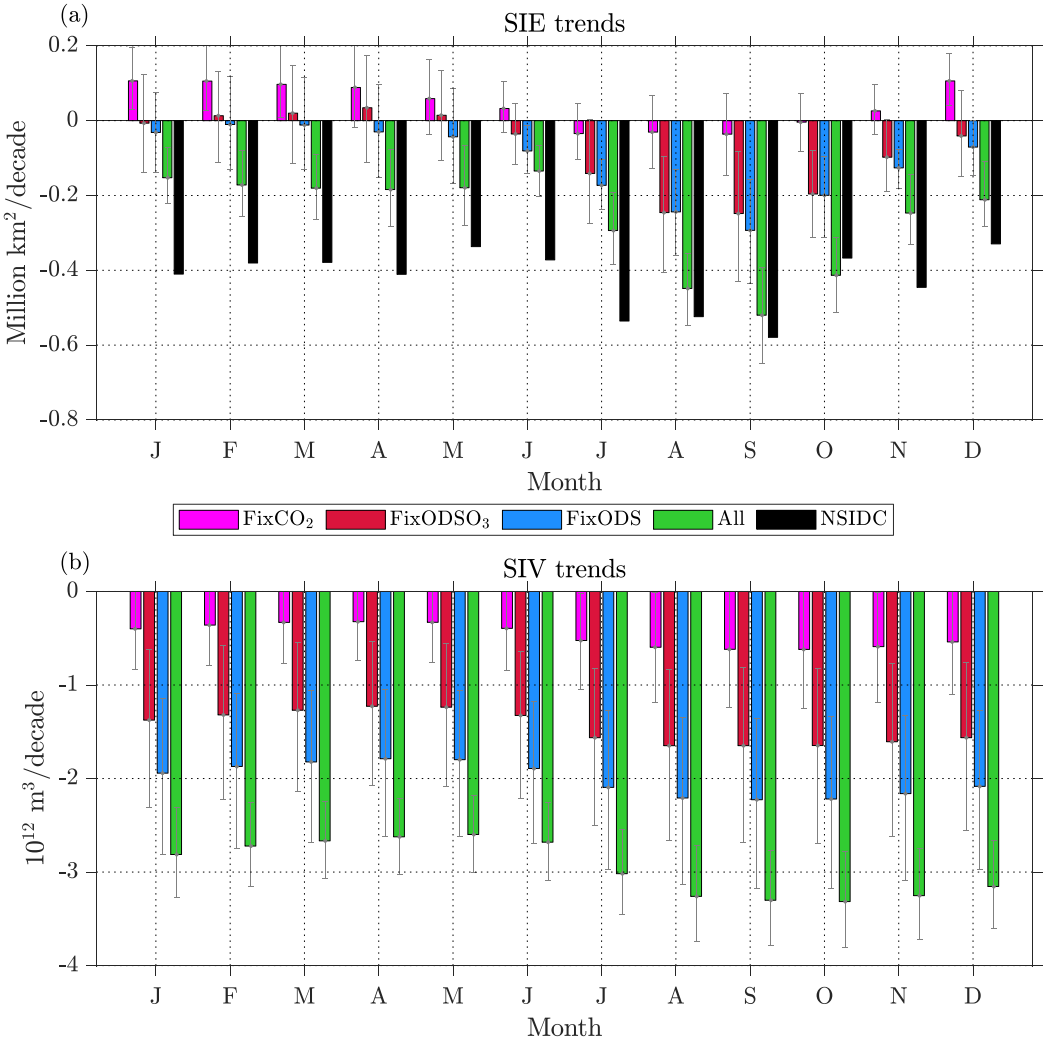

Figure 2. Observed (black bars) and simulated (colored bars) monthly trends in (a) pan-Arctic SIE and (b) pan-Arctic SIV computed over the period 1979–2005 in the All forcing (green), FixODS (blue), FixODSO$_3$ (red), and FixCO$_2$ (magenta) simulations. The bars show the ensemble-mean trends and error bars indicate the 95% confidence range for the ensemble-mean trends, obtained by bootstrapping the ensemble.

3.2. Physical processes contributing to sea ice trend differences

Next, we consider the physical processes responsible for the trend differences identified in the fixed CO_2 and ODS experiments. We first analyze trends in sea ice mass budget tendency terms. The sea ice mass budget consists of a dynamic tendency term (ice mass transport convergence) and a thermodynamic tendency term (ice melt and growth). All terms use a sign convention with positive values corresponding to mass gain and negative values correspond to mass loss. In figure 4, we compute mass budgets over a Central Arctic basin domain consisting of the Central Arctic, Canadian Arctic Archipelago, Kara, Laptev, East Siberian, Chukchi, and Beaufort Seas, following the regional definitions of Bushuk *et al* (2017) (see inset in figure 4(e)). This analysis domain spans the region of thickest Arctic sea ice and its boundaries encompass all flux gates through which ice passes into the North Atlantic and North Pacific sectors. The mass budget terms are computed as areal integrals over the analysis domain, following the approach used in the mass budget intercomparison study of Keen *et al* (2021). We also plot summer and winter spatial trends of mass budget terms in figures 5 and S2, respectively.

We find that the sea ice trend differences across experiments are dominated by differences in thermodynamic, rather than dynamic, sea ice processes (figures 4(a) and (b); figures 5(a) and (b)). In particular, the All forcing run has the strongest trend towards increased summer melt and these melt trends are correspondingly reduced in the runs with Fixed ODS and CO_2. The melt changes due to ODS represent 57% of the melt changes due to CO_2. The melt trend differences are due to both top melt and basal melt, with these terms making roughly equal contributions to the summer melt differences across experiments

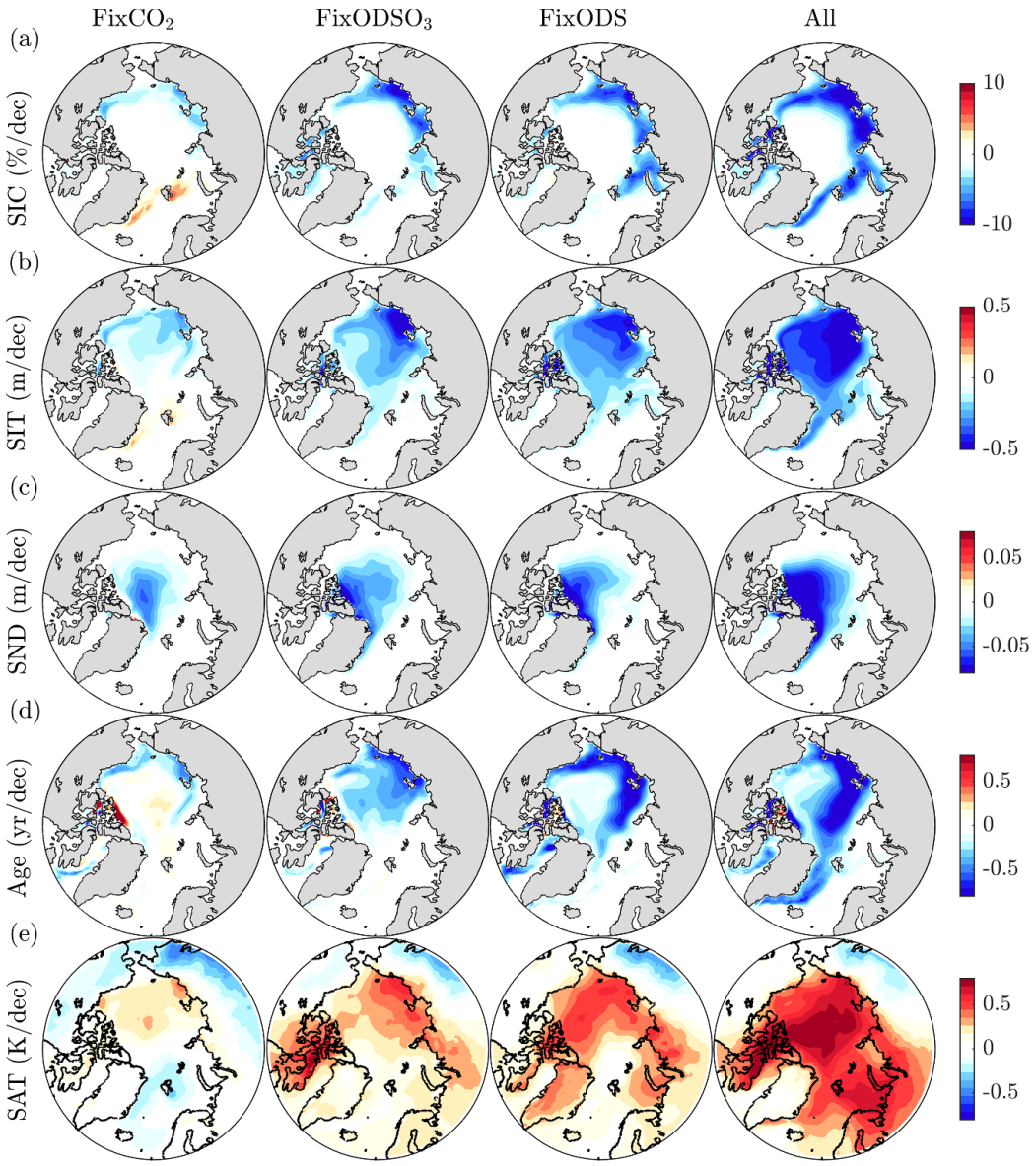

Figure 3. Ensemble-mean summer (July-August-September) trends in sea ice concentration (% decade^{-1}; row (a)), sea ice thickness (m decade^{-1}; row (b)), snow depth (m decade^{-1}; row (c)), sea ice age (years decade^{-1}; row (d)), and surface air temperature (K decade^{-1}; row (e)) in the CESM FixCO$_2$, FixODSO$_3$, FixODS, and All forcing simulations.

(figures 4(c) and (d); figures 5(c) and (d)). The lateral melt term and its trends are small in all experiments (figure 4(e)), consistent with the findings of Keen *et al* (2021).

The summer melt differences are broad-scale, occurring across the Central Arctic (figures 5(b)–(d)), and closely mirroring the SIT differences in figure 3(b). Note that the ring of positive melt trends at the sea ice periphery occurs due to the negative trends in SIT—there is simply less sea ice mass available to melt at those locations. The spatial changes associated with ice dynamics are noisier (figure 5(a)) and essentially cancel when integrated over the Central Arctic basin domain. There is an increasingly positive trend from ice dynamics in the Central Arctic as one moves across figure 5(a) from the fixed CO$_2$ to the All forcing run. This is possibly due to the fact that ice strength decreases as ice thins, making it easier to import ice into the Central Arctic, which is typically a region of ice convergence.

The trends towards greater summer melt are partially, but not completely, offset by trends towards greater sea ice growth in autumn and winter months (November–March; figure 4(b)). This increased winter ice growth is consistent with a stronger negative ice thickness-growth feedback, associated with the thinning trends in these simulations (Bitz and Roe 2004, Petty *et al* 2018). As expected from this negative feedback, we find the largest winter ice growth increase in the All forcing simulations, followed by the FixODS and FixCO$_2$

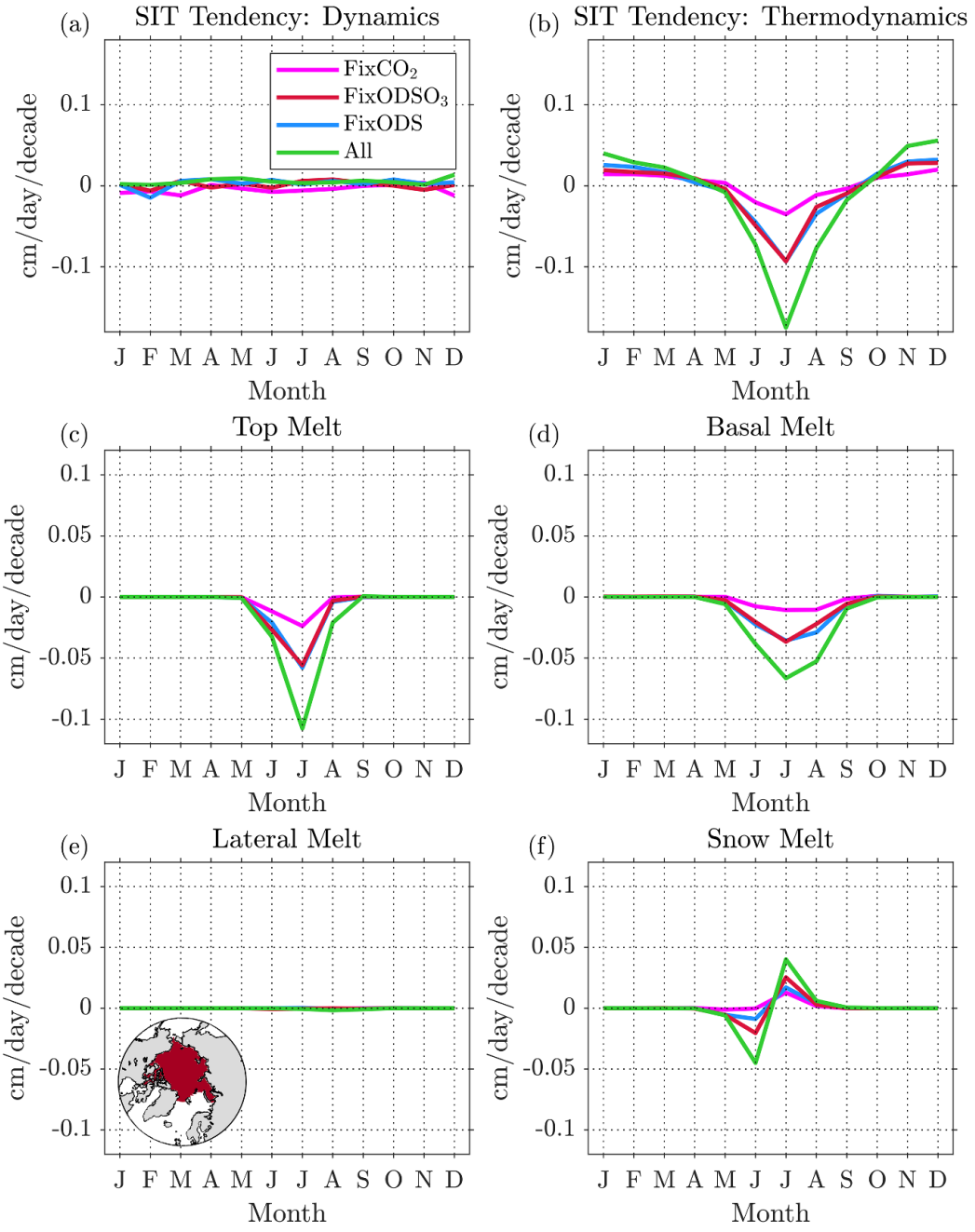

Figure 4. Sea ice mass budget monthly trends averaged over the Central Arctic basin in the $FixCO_2$ (magenta), $FixODSO_3$ (red), FixODS (blue), and All forcing (green) simulations. Panels (a) and (b) show SIT tendency trends due to dynamic and thermodynamic processes, respectively. Panels (c)–(e) show SIT tendency trends due to top, basal, and lateral melt, respectively. Panel (f) shows SND tendency trends. Positive values correspond to mass gain and negative values correspond to mass loss. The Central Arctic basin domain used for analysis is shown in the inset in panel (e).

simulations, respectively. The growth differences have a broad scale pattern that closely resembles the winter thickness differences between simulations (compare figure S2(b) to figure S1(b)). We also find that snow melt on sea ice increases in the month of June and decreases in the month of July in all experiments, indicating a shift of snow melt to earlier in the summer season (figure 4(f)). This snow melt shift is largest in the All forcing experiments, and is progressively smaller in the FixODS and $FixCO_2$ simulations, respectively. Note that in these simulations, all snow on sea ice melts eventually over the summer. This explains the decreases in July snow melt—there is less snow mass available to melt in July due to the increased snow melt that occurred in June. The key point revealed by this sea ice mass budget analysis is that the impact of ODS on sea ice is similar to that of CO_2, only smaller in magnitude owing to its smaller radiative forcing.

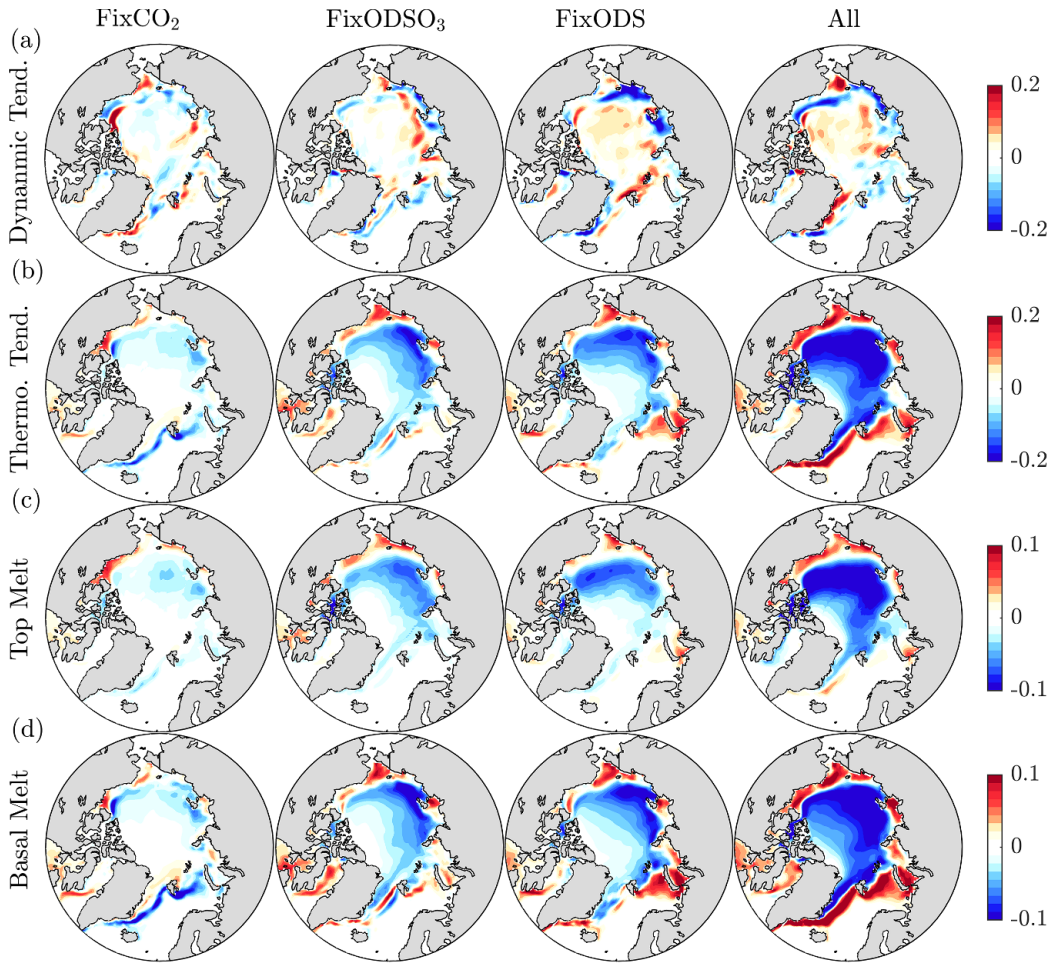

Figure 5. Ensemble-mean summer (July–August–September) trends in SIT tendency trends due to dynamic processes (row (a)), thermodynamic processes (row (b)), top melt (row (c)), and basal melt (row (d)) in the CESM FixCO$_2$, FixODSO$_3$, FixODS, and All forcing simulations. All terms have units of cm day^{-1} decade^{-1}, with positive values corresponding to mass gain and negative values corresponding to mass loss.

We have attributed the stronger trends in the All forcing simulations to increased summer melt relative to the fixed ODS and CO$_2$ runs. Next, we consider the drivers of this increased summer melt. In figure 6(a), we plot annual-mean trends of surface energy budget terms averaged over an Arctic domain north of 60° N. All terms are defined as positive downwards, with positive fluxes contributing to surface warming and sea ice melt. We find consistent mechanisms of Arctic warming present across the experimental suite, with surface energy budget trends that are ordered according to their Arctic SAT trends. These SAT trends are largest in the All forcing run, followed by the FixODS, FixODSO$_3$, and FixCO$_2$ runs, respectively.

We find that the two key drivers of surface Arctic warming are increased downwelling longwave radiation and decreased upwelling shortwave radiation, consistent with earlier work (e.g. Boeke and Taylor 2018). Relative to the All forcing run, the fixed ODS and CO$_2$ runs have reduced downwelling longwave radiation due to their reduced GHG-based radiative forcing, with the ODS impact representing 35% of the CO$_2$ impact. The fixed ODS and CO$_2$ runs also have notable reductions in upwelling shortwave radiation. These reductions are consistent with the increased sea ice cover in these runs, which increases the surface albedo and produces more reflected shortwave radiation. In particular, the ODS impact on upwelling shortwave is 44% that of CO$_2$, which closely reflects their relative impacts on surface albedo and SIE trends, which are 43% and 50%, respectively.

The upwelling longwave and downwelling shortwave heat fluxes each provide notable negative feedbacks which oppose this Arctic warming. The upwelling longwave trends act to cool the surface via the Planck feedback, and closely resemble the negative of the Arctic SAT trends. Consistent with this, the relative impact of ODS on upwelling longwave radiation and SAT are 35% and 35% of the CO$_2$ impacts, respectively. We also find systematic increases in downwelling shortwave radiation in the fixed forcing experiments. These

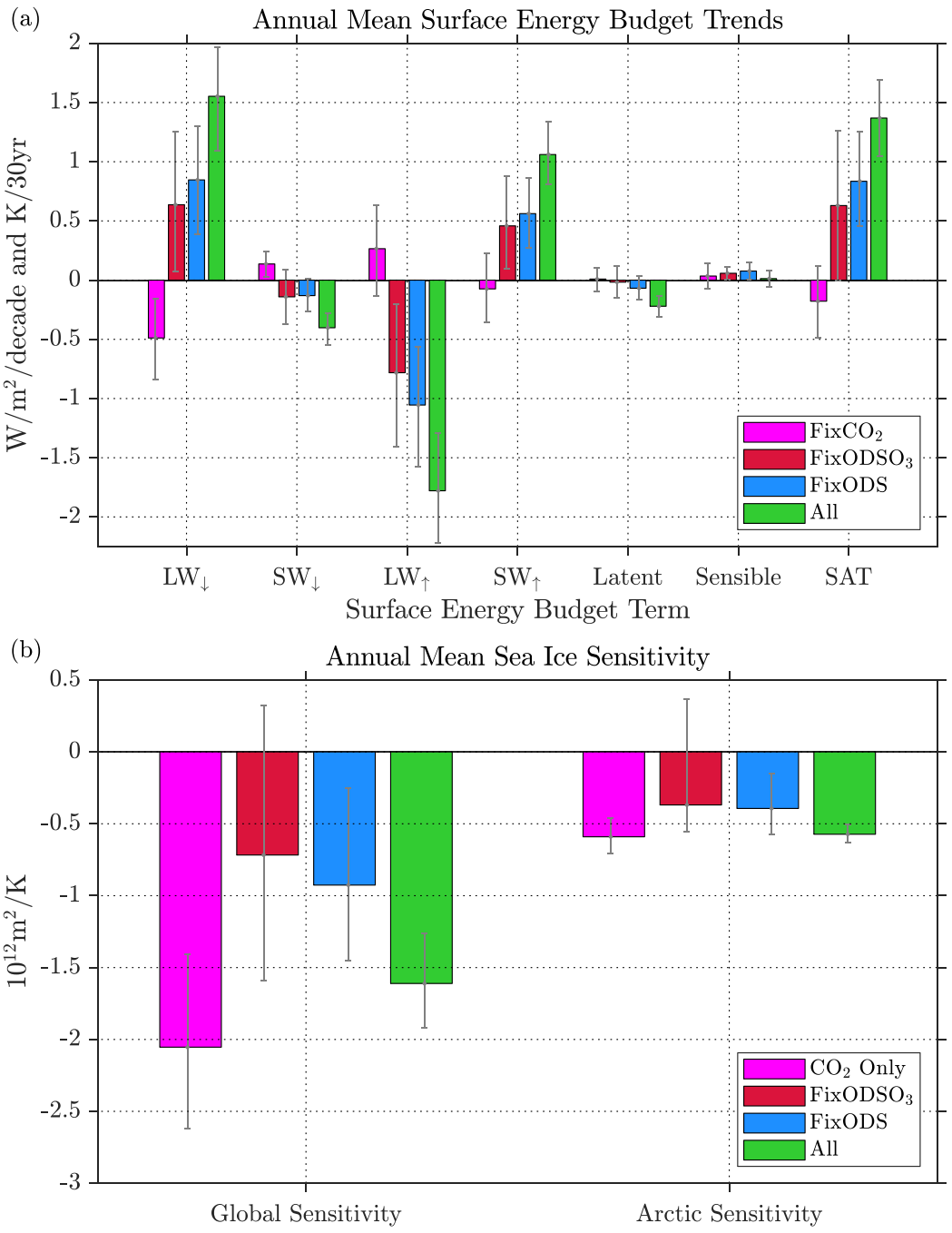

Figure 6. (a): Annual mean trends in surface energy budget terms averaged over the Arctic region in the FixCO$_2$ (magenta), FixODSO$_3$ (red), FixODS (blue), and All forcing (green) simulations. All terms are defined as positive downwards (positive fluxes contribute to surface warming). The SAT column indicates the trend in SAT in units of K/30 years. (b): Arctic SIE sensitivity to global-mean and Arctic-mean surface temperatures (defined as the ratio of annual-mean SIE trends to annual-mean temperature trends). Error bars indicate the 95% confidence range for the ensemble-mean trends and sensitivities, obtained by bootstrapping the ensemble.

increases are consistent with increased multiple reflections off clouds due to the increased sea ice cover and surface albedo in these runs (Wendler *et al* 1981). Indeed, we find that the fixed ODS runs provide 50% the impact of CO_2 on downwelling shortwave radiation, which generally reflect their relative impacts on surface albedo and SIE (43% and 50%, respectively). Compared to the radiative flux terms, the contributions from latent and sensible heat fluxes are relatively modest. But, again, the key point is that ODS impact the same surface energy budget terms as CO_2, only with a smaller amplitude.

Finally, we consider whether ODS influence the sensitivity of Arctic sea ice to surface temperature warming, a quantity evaluated by many prior studies (e.g. Gregory *et al* 2002, Winton 2011, Mahlstein and

Knutti 2012, Rosenblum and Eisenman 2017, SIMIP Community 2020, Bonan *et al* 2021). In figure 6(b), we plot the ratio of annual-mean Arctic SIE trends to annual-mean surface temperature trends across the experimental suite. The surface temperatures are averaged either globally or over an Arctic domain north of 60° N, and ensemble means are computed prior to taking the ratio. Note that reliable sensitivities could not be computed for the FixCO_2 run because temperature trends are close to zero in this experiment, and thus the sensitivity metric is poorly conditioned. Therefore, we instead consider a 'CO_2 Only' sensitivity, based on trend differences between the All forcing and FixCO_2 runs. This difference has large trends in both SIE and temperature, allowing for a robust computation of sensitivity to CO_2 forcing alone.

We find that Arctic SIE sensitivity to global-mean surface temperature (GMST) is lower in the runs that fix ODS compared with the All forcing and CO_2 Only sensitivities. In both the FixODS and Fix$ODSO_3$ runs, the sensitivity differences are significant at the 95% level relative to both CO_2 Only and All forcing. This lower sensitivity to GMST in fixed ODS runs is consistent with the earlier results of Liang *et al* (2022) and Sigmond *et al* (2023), who found that ODS forcing produces greater Arctic Amplification than CO_2 forcing. The SIE sensitivity to Arctic temperatures is more consistent across experiments. The fixed ODS runs have slightly lower sensitivity than CO_2 Only and All forcing, but the differences are generally not significant at the 95% level, with the exception being the difference between the FixODS and All forcing runs. Our finding that sea ice sensitivity to GMST depends on the forcing agents considered emphasizes the fact that historical sea ice sensitivity needs to be evaluated using realistic historical forcings, consistent with the recent results of DeRepentigny *et al* (2022).

4. Discussion and conclusions

Using all-but-one-forcing ensembles, we have investigated the role that ODS have played in historical Arctic sea ice loss and have placed this ODS impact in the context of CO_2 forcing. We have found that ODS forcing played a significant role in year-round SIE and SIV trends over the second half of the 20th century, with SIE and SIV trends reduced by 64% and 32%, respectively, when the impacts of ODS are removed. These ODS trend contributions represent a substantial fraction (50% and 38%, respectively) of the sea ice loss from CO_2 forcing. We found that ODS, like CO_2, affect sea ice by thermodynamic rather than dynamic sea ice processes, and that the losses in both cases can be attributed to summer sea ice melt. These melt differences are dominated by changes in downwelling longwave radiation associated with GHG radiative forcing and changes in upwelling shortwave radiation associated with sea ice and surface albedo changes.

We note that the impact of ODS on sea ice loss compared to CO_2 in this model appears to be larger than would be expected from global mean radiative forcing alone (Meinshausen *et al* 2011). Relatedly, we have also found that the sensitivity of Arctic sea ice to global-mean surface temperature change is larger when ODS forcing is included. These findings suggest that ODS might be more efficient than CO_2 at causing Arctic sea ice loss. However, since we do not have the actual radiative forcings over the Arctic for our model over the period of interest (1955–2005), we are unable to explore this question further at this time. We plan new dedicated runs to compute the separate surface and top-of-atmosphere radiative forcings over the Arctic to better quantify this potentially important effect.

Finally, we emphasize the remarkable fact that the Montreal Protocol, originally designed to halt the formation of the ozone hole over the Antarctic, has resulted in a substantial reduction of sea ice loss in the Arctic (England and Polvani 2023). Given the different time evolution of GHG forcing agents, it is important to move beyond sole consideration of CO_2 and also consider the influence of non-CO_2 GHG forcing agents in historical Arctic sea ice evolution. This may be especially important for ODS since (i) they exhibit a highly distinct and non-monotonic forcing history compared to CO_2 and (ii) they may have a high efficacy in causing Arctic sea ice loss, which would make their contribution larger than previously expected. Therefore, consideration of ODS forcing trajectories will likely be critical in understanding both past and future sea ice changes. It is also crucial to note that the results of this study are based upon a single model. The recent study of Sigmond *et al* (2023) found a similar response to ODS forcing in the CanESM5 model, but similar experiments with other climate models are required to build confidence in these findings, particularly using CMIP6 historical forcings which will allow for results to be extended to the end of 2014.

Data availability statement

The CESM-LE data are available for download from the Earth System Grid Federation data portal (www.cesm.ucar.edu/projects/community-projects/LENS/data-sets.html). The CESM all-but-one-forcing experiment data and analysis code are available via a Zenodo repository (https://zenodo.org/record/7469290). The NASA team sea ice concentration observations used in this study are available from the National Snow and Ice Data Center website (http://nsidc.org/data/NSIDC-0051/versions/1).

Acknowledgments

We acknowledge the CESM Large Ensemble Community Project, which is supported by the National Science Foundation (NSF). Five of the CESM-LE simulations were produced at the University of Toronto under the supervision of Paul Kushner.

We thank two anonymous reviewers for constructive comments that improved the manuscript. We thank Alexander Huth and Nadir Jeevanjee for comments on a preliminary version of the manuscript. Mitch Bushuk's research at the Geophysical Fluid Dynamics Laboratory was supported by NOAA's Science Collaboration Program and administered by UCAR's Cooperative Programs for the Advancement of Earth System Science (CPAESS) under Awards NA16NWS4620043 and NA18NWS4620043B.

ORCID iDs

Mitchell Bushuk https://orcid.org/0000-0002-0063-1465
Lorenzo M Polvani https://orcid.org/0000-0003-4775-8110
Mark R England https://orcid.org/0000-0003-3882-872X

References

Bitz C and Roe G 2004 A mechanism for the high rate of sea ice thinning in the Arctic Ocean *J. Clim.* **17** 3623–32
Boeke R C and Taylor P C 2018 Seasonal energy exchange in sea ice retreat regions contributes to differences in projected Arctic warming *Nat. Commun.* **9** 1–14
Bonan D B, Schneider T, Eisenman I and Wills R C J 2021 Constraining the date of a seasonally ice-free Arctic using a simple model *Geophys. Res. Lett.* **48** e2021GL094309
Bushuk M, Msadek R, Winton M, Vecchi G, Gudgel R, Rosati A and Yang X 2017 Skillful regional prediction of Arctic sea ice on seasonal timescales *Geophys. Res. Lett.* **44** 4953–64
Cavalieri D J, Parkinson C L, Gloersen P and Zwally H J 1996 Sea ice concentrations from Nimbus-7 SMMR and DMSP SSM/I-SSMIS passive microwave data, version 1 *NASA DAAC at the National Snow and Ice Data Center* (https://doi.org/10.5067/8GQ8LZQVL0VL)
DeRepentigny P *et al* 2022 Enhanced simulated early 21st century Arctic sea ice loss due to CMIP6 biomass burning emissions *Sci. Adv.* **8** eabo2405
Deser C *et al* 2020 Insights from Earth system model initial-condition large ensembles and future prospects *Nat. Clim. Change* **10** 277–86
Ding Q *et al* 2019 Fingerprints of internal drivers of Arctic sea ice loss in observations and model simulations *Nat. Geosci.* **12** 28
England M R and Polvani L M 2023 The Montreal Protocol is delaying the occurrence of the first ice-free Arctic summer *Proc. Natl Acad. Sci.* **120** e2211432120
England M, Jahn A and Polvani L 2019 Nonuniform contribution of internal variability to recent Arctic sea ice loss *J. Clim.* **32** 4039–53
Fyfe J C, von Salzen K, Gillett N P, Arora V K, Flato G M and McConnell J R 2013 One hundred years of Arctic surface temperature variation due to anthropogenic influence *Sci. Rep.* **3** 2645
Garcia R R, Kinnison D E and Marsh D R 2012 World avoided simulations with the whole atmosphere community climate model *J. Geophys. Res. Atmos.* **117** D23303
Goyal R, England M H, Gupta A S and Jucker M 2019 Reduction in surface climate change achieved by the 1987 Montreal Protocol *Environ. Res. Lett.* **14** 124041
Gregory J M, Stott P, Cresswell D, Rayner N, Gordon C and Sexton D 2002 Recent and future changes in Arctic sea ice simulated by the HadCM3 AOGCM *Geophys. Res. Lett.* **29** 28–21
Hansen J, Lacis A and Prather M 1989 Greenhouse effect of chlorofluorocarbons and other trace gases *J. Geophys. Res. Atmos.* **94** 16417–21
Hurrell J W *et al* 2013 The Community Earth System model: a framework for collaborative research *Bull. Am. Meteorol. Soc.* **94** 1339–60
Intergovernmental Panel on Climate Change (IPCC) 2023 Ocean, cryosphere and sea level change, in climate change 2021—the physical science basis: working group I contribution to the sixth assessment report of the intergovernmental panel on climate change *Technical Report* (Cambridge University Press) pp 1211–362
Kay J E *et al* 2015 The Community Earth System Model (CESM) large ensemble project: a community resource for studying climate change in the presence of internal climate variability *Bull. Am. Meteorol. Soc.* **96** 1333–49
Kay J E, Holland M M and Jahn A 2011 Inter-annual to multi-decadal Arctic sea ice extent trends in a warming world *Geophys. Res. Lett.* **38** L15708
Keen A *et al* 2021 An inter-comparison of the mass budget of the Arctic sea ice in CMIP6 models *Cryosphere* **15** 951–82
Kong N and Liu W 2023 Unraveling the Arctic sea ice change since the middle of the twentieth century *Geosciences* **13** 58
Li D, Zhang R and Knutson T R 2017 On the discrepancy between observed and CMIP5 multi-model simulated Barents Sea winter sea ice decline *Nat. Commun.* **8** 14991
Liang Y-C, Polvani L M, Previdi M, Smith K L, England M R and Chiodo G 2022 Stronger Arctic amplification from ozone-depleting substances than from carbon dioxide *Environ. Res. Lett.* **17** 024010
Mahlstein I and Knutti R 2012 September Arctic sea ice predicted to disappear near 2 °C global warming above present *J. Geophys. Res. Atmos.* **117** D06104
Meinshausen M *et al* 2011 The RCP greenhouse gas concentrations and their extensions from 1765 to 2300 *Clim. Change* **109** 213–41
Meredith M *et al* 2019 Polar regions *Ipcc Special Report on the Ocean and Cryosphere in a Changing Climate*, ed H -O Pörtner *et al* (Cambridge University Press) pp 203–320
Montzka S A, Dlugokencky E J and Butler J H 2011 Non-CO_2 greenhouse gases and climate change *Nature* **476** 43–50
Morgenstern O, Braesicke P, Hurwitz M M, O'Connor F M, Bushell A C, Johnson C E and Pyle J A 2008 The world avoided by the Montreal Protocol *Geophys. Res. Lett.* **35** L16811
Notz D 2015 How well must climate models agree with observations? *Phil. Trans. R. Soc.* A **373** 20140164

Petty A A, Holland M M, Bailey D A and Kurtz N T 2018 Warm Arctic, increased winter sea ice growth? *Geophys. Res. Lett.* **45** 12–922
Polvani L M, Camargo S J and Garcia R R 2016 The importance of the Montreal Protocol in mitigating the potential intensity of tropical cyclones *J. Clim.* **29** 2275–89
Polvani L M, Previdi M, England M R, Chiodo G and Smith K L 2020 Substantial twentieth-century Arctic warming caused by ozone-depleting substances *Nat. Clim. Change* **10** 130–3
Polvani L M, Waugh D W, Correa G J P and Son S-W 2011 Stratospheric ozone depletion: the main driver of twentieth-century atmospheric circulation changes in the Southern Hemisphere *J. Clim.* **24** 795–812
Prather M J, Zhu X, Tang Q, Hsu J and Neu J L 2011 An atmospheric chemist in search of the tropopause *J. Geophys. Res. Atmos.* **116** D04306
Ramanathan V 1975 Greenhouse effect due to chlorofluorocarbons: climatic implications *Science* **190** 50–52
Rosenblum E and Eisenman I 2017 Sea ice trends in climate models only accurate in runs with biased global warming *J. Clim.* **30** 6265–78
Sigmond M, Polvani L, Fyfe J, Smith C, Cole J and England M 2023 Large contribution of ozone-depleting substances to global and Arctic warming in the late 20th century *Geophys. Res. Lett.* **50** e2022GL100563
SIMIP Community 2020 Arctic sea ice in CMIP6 *Geophys. Res. Lett.* **47** e2019GL086749
Solomon S 1999 Stratospheric ozone depletion: a review of concepts and history *Rev. Geophys.* **37** 275–316
Stroeve J, Kattsov V, Barrett A, Serreze M, Pavlova T, Holland M and Meier W N 2012 Trends in Arctic sea ice extent from CMIP5, CMIP3 and observations *Geophys. Res. Lett.* **39** L16502
Stroeve J and Notz D 2018 Changing state of Arctic sea ice across all seasons *Environ. Res. Lett.* **13** 103001
Swart N C, Fyfe J C, Hawkins E, Kay J E and Jahn A 2015 Influence of internal variability on Arctic sea-ice trends *Nat. Clim. Change* **5** 86–89
Velders G J M, Andersen S O, Daniel J S, Fahey D W and McFarland M 2007 The importance of the Montreal Protocol in protecting climate *Proc. Natl Acad. Sci.* **104** 4814–9
Wendler G, Eaton F D and Ohtake T 1981 Multiple reflection effects on irradiance in the presence of Arctic stratus clouds *J. Geophys. Res. Oceans* **86** 2049–57
Winton M 2011 Do climate models underestimate the sensitivity of Northern Hemisphere sea ice cover? *J. Clim.* **24** 3924–34
World Meteorological Organization 2018 Scientific assessment of ozone depletion: 2018, global ozone research and monitoring project—report no. 58 *Technical Report* pp 1–588
Young P *et al* 2013 Pre-industrial to end 21st century projections of tropospheric ozone from the Atmospheric Chemistry and Climate Model Intercomparison Project (ACCMIP) *Atmos. Chem. Phys.* **13** 2063–90